Research on a Bionic Ray Robot and its Control Method based on CPG

Ying Zhang, Guifang Qiao, Di Liu, Yihan Sun

Abstract—The ray is a typical template for developing bionic robot fish, because of their distinctive undulating motion powered by their pectoral fins. This paper presents the design of a bionic ray robot, which imitates the movements of real rays. Firstly, the kinematics model is established by analyzing biological characteristics. A bionic ray robot is designed by using the swing mechanism as the skeleton of the simulated pectoral fin. Secondly, a control strategy based on a double-layered central pattern generator (CPG) is proposed. This approach employs a rhythm layer controlled by Kuramoto oscillator to modulate the traditional single-layer, semi-central structure-based pattern layer. By fine-tuning the parameters of the CPG model, diverse motion modes of the ray robot can be controlled effectively. Finally, the double-layered CPG motion control approach has been confirmed feasible through simulations and practical experiments. In order to further validate the effectiveness, an experimental prototype was developed, which is equipped with Bluetooth remote controller and a water quality detection module. The simulations were conducted in a wave-free environment created in Webots software. Three different motion modes were displayed by the ray robot prototype: straight movement, turning movement, and diving movement. The performances of the movements of the robot were analyzed. The results demonstrate that the developed double-layered CPG motion control method not only improves the multi-modal motion ability of the ray robot, but also exhibits good robustness.

***Index Terms*—bionic ray robot, multi-joint swinging mechanism, double-layered CPG network, motion control**

I. Introduction

THE ocean is a vast reservoir of energy, teeming with diverse biological life and rich metallic resources. Underwater exploration using robotic technology can reduce the risks and human resource consumption caused by long-term operations in challenging marine environment [1]. Through hundreds of millions of years of natural evolution, aquatic species have honed their extraordinary adaptations to the complex underwater environments. The fish propelled by pectoral fin is better than other fish in stability, concealment ability and low energy consumption [2]. As a typical case, the bionic ray robot has become a hot research topic in the field of underwater robots in recent years [3-5].

The propulsion modes of fish are categorized into body/caudal fin (BCF) propulsion and median/paired fin (MPF) propulsion [6,7]. BCF propulsion represents the predominant method used by fish. The fish generates propulsion by swinging the body and caudal fin, making it suitable for continuous high-speed cruising [8]. MPF propulsion mainly relies on the oscillation of median fin or paired fin to generate thrust, aiming at enhancing the mobility and stability during swimming, while maintaining balance. Therefore, many fish use MPF propulsion as an auxiliary propulsion mechanism to enhance their flexibility [9]. BCF-driven bionic robotic fish exhibit remarkable propulsive performance [10]. Barrett et al. pioneered the development of the bionic fish prototype modeled after the bluefin tuna, which was propelled by caudal fin, and the swimming speed per second could reach 0.5 times its body length [11]. Zhou et al. later succeeded in developing the RoMan-II robotic ray [12], integrating a CPG-based motion control system with six oscillators to manage the movement of six fins, so as to obtain the required swimming gaits. On the basis of RoMan-II design, they further designed RoMan-III ray robot [13]. The team delved into various factors that affect the fin propulsion of RoMan-III, such as swing amplitude, frequency and fin area. They also optimized the structural design and motion control approach. Chen et al. [14] utilized ion-exchange polymer metal composites to craft bionic ray pectoral fins, allowing for propulsion through the activation of a single IPMC, thus simplifying the control strategy for autonomous swimming. Glushko et al. [15] explored the capabilities of a bionic ray robot with multi-mode propulsion. Cai Y et al. [16] designed an innovative bionic propulsion fin strip actuated by a multi-joint mechanism, composed of a synchronous belt mechanism and a slider-rocker mechanism.

In recent years, CPG has been widely used to control bionic robots [17-19]. In the control of bionic fish, CPG can coordinate the free switching of various swimming modes, so it has attracted much attention [20,21]. Wang et al. [22] developed a dynamic model for robotic fish by combining the Newton-Euler method and a bionic CPG controller. A four-oscillator CPG network model was employed to generate coordinated control signals for the swinging joints. Nguyen et al. [23] introduced a CPG network consisting of sixteen coupled Hopf oscillators for gait generation to complete fishlike swimming motions. The CPG network was optimized by using a differential particle swarm optimization technology to improve the thrust force and avoid local maxima, thus improving the propulsion performance of the

Manuscript received July 7, 2024; revised December 21, 2024.

This work was supported in part by the Natural Science Foundation of China under Grant 51905258, China Postdoctoral Science Foundation 2019M650095, and Scientific Research Funds of Nanjing Institute of Technology CKJB202104.

Ying Zhang is a lecturer in the School of Automation, Nanjing Institute of Technology, Nanjing 211167, P.R. China (email: zhangying295@126.com).

Guifang Qiao is an associate professor in the School of Automation, Nanjing Institute of Technology, Nanjing 211167, P. R. China (email: qiaoguifang@126.com).

Di Liu is a professor in the School of Automation, Nanjing Institute of Technology, Nanjing 211167, P. R. China (email: zdhxld@njit.edu.cn).

Yihan Sun is a postgraduate student in the School of Advanced Technology, Xi'an Jiaotong-Liverpool University, Suzhou 215123, P. R. China (email: 1115398285@qq.com).

undulating fin robot. Zhang et al. [24] designed a bionic CPG network for a finfish robot, enabling motion modes including straight and steering swimming. Koca et al. [25] proposed a finite state machine (FSM) algorithm that successfully implemented autonomous obstacle avoidance control and three-dimensional motion control during the yawing process of the bionic fish by integrating CPG with a fuzzy controller.

In this paper, a bionic ray robot is designed inspired by the natural characteristics of the rays, and the motion control method is investigated. Firstly, the biological model of the ray is analyzed, and the simplified physical model and kinematic model are established, and the mechanical structure of the bionic ray robot is designed. Secondly, the role of the CPG network in enhancing the motion control ability of the ray robot is studied. A double-layered CPG network model is constructed using Simulink. By fine-tuning some parameters within the model, the ray robot can execute three different motion modes. Finally, the bionic ray model crafted in Solidworks software is integrated into the Webots software. This integration allows for joint simulation with MATLAB, thus verifying the feasibility and effectiveness of the established CPG network model for the motion control method of the bionic ray robot.

II. Mechanism Design of the Bionic Ray Robot

Rays possess a large and streamlined flat body curve, which looks like a diamond shape from above. Within their pectoral fins, there are radiating fins composed of calcified hard bones and cartilage, which are integrated with the muscles and flexible body. This structure endows the pectoral fins with excellent compound flexibility, allowing them to flexibly control their deformation and movement [26]. The rays are capable of executing various swimming movements, including straight movement, turning movement, and diving movement. By swinging their pectoral fins synchronously or asynchronously, they are consistent with the swinging of caudal fin and the flexible fluctuation of their body. From the bionics perspective, the structure of the ray pectoral fin can be divided into the pectoral fin skeleton and the pectoral fin flexible epidermis. These two components work in coordination to realize the motion functions of the bionic pectoral fin.

A. Kinematics model of the biological ray

The ray pectoral fin can be modeled as a thin flexible plate, and its coordinate system is set up as depicted in Fig. 1. The base line of the pectoral fin is taken as the *x*-axis, the intersection point of the base line and the leading edge is taken as the origin *O*, and the plane where the pectoral fin is fully extended is defined as y=0. Then, the *z*-axis is determined by applying the right-handed rule.

When the pectoral fin moves vertically up and down, the *y*-axis can be used to track the swing amplitude of the pectoral fin. Similarly, the *z*-axis is instrumental in charting the longitudinal variation in amplitude. According to this comprehensive analysis, the kinematic equation of the bionic ray is as follows.

$$\begin{cases} y = A(z)\sin(kx-\omega t) \\ k = 2\pi/\lambda \\ \omega = 2\pi f \end{cases} \tag{1}$$

where x, y, and z represent the spatial coordinates of any given point on the pectoral fin. $A(z)$ represents the amplitude control factor, which the a function of z and has a related sub-amplitude control factor at its peak power. λ denotes the wavelength of the traveling wave. f stands for the swing frequency of the pectoral fin, and t signifies swing time. The coordinates of any point on the pectoral fin are dynamically influenced by the movement of the ray over time, following the principles of sinusoidal change. This change is closely related to the wavelength λ and the swing frequency f.

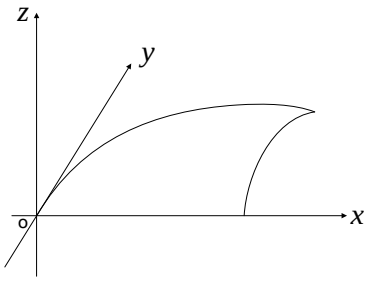

Fig. 1. The coordinate system of the pectoral fin

B. Mechanical structure design of the bionic ray robot

The mechanical design of the ray robot should consider the biological characteristics of a biological ray. The whole structure of the ray robot is crafted to resemble a flat shape. Pectoral fins generate propulsion through extensive swing amplitudes during swimming while the caudal fin adjusts posture for balance maintenance. As shown in Fig. 2, the bionic ray robot is mainly composed of body, pectoral fins and caudal fin. The upper and lower surfaces of the fish are outlined by arc-shaped parts to mimic the natural curvature of a biological ray. There is a hollow installation space inside the robot body, which can be used to install and fix necessary development boards, various sensors, wiring connections and other equipment.

Taking one side of the pectoral fin as an example, the pectoral fin assembly is composed of an array of articulated swing mechanisms. The multi-joint swinging mechanism consists of three steering gears connected by their corresponding brackets. Each steering gear represents a part of the joint skeleton. The joint swing mechanism of the pectoral fin is shown in Figure 3. Each joint swing mechanism is actuated by a steering gear, facilitating a vertical swinging motion that drives the propulsion of the ray robot. The connecting bracket is designed with an *L*-shaped structure. One end is fixed on the multifunctional bracket, while the other end is connected to a *U*-shaped bracket to ensure the connectivity between joints and maintaining the structural integrity of the fin.

The caudal fin is composed of a caudal steering mechanism and a caudal plate, as shown in Fig. 4. The caudal steering gear is enclosed by a cover plate fixed between the inside of the fuselage and the control panel to adjust the vertical movement of the caudal plate. By adjusting the

movement of the caudal fin, effective adjustment of the center of gravity can be realized to prevent problems such as uncontrolled movements. Because the caudal fin does not generate active propulsion, it mainly maintains the stability of the robot through the slight oscillations during swimming. In the design of the tail fin, only one steering gear is employed to simulate vertical swings of the caudal fin.

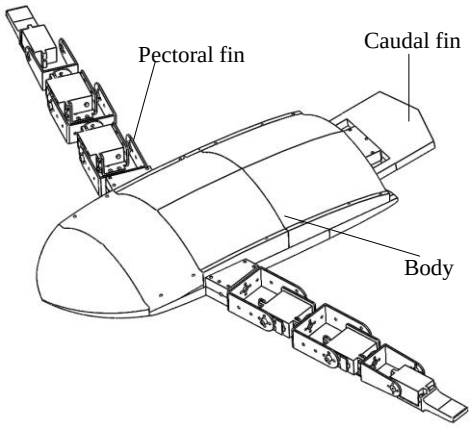

Fig. 2. The model of the bionic ray robot

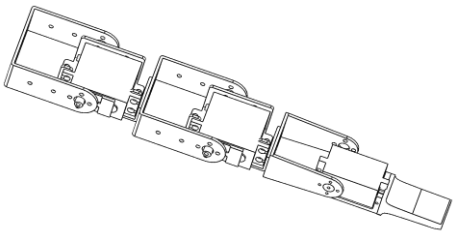

Fig. 3. The joint swing mechanism of the pectoral fin

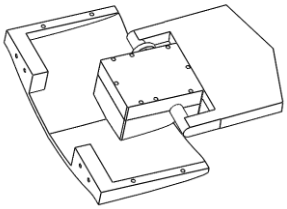

Fig. 4. The joint swing mechanism of the caudal fin

III. The Design of Bionic Ray Robot Control System

As shown in Fig. 5, the overall control system mainly consists of an Arduino control panel and auxiliary modules, including a 7-way steering gear, a water quality sensor module, a Bluetooth communication module and a power supply module. The steering gears are responsible for driving the left and right pectoral fins, and the caudal fin of the bionic ray robot. Arduino control panel exerts commands over each steering gear through PWM signals to achieve diverse motion modes. Additionally, the Arduino control panel establishes communication with MATLAB via the communication module, ensuring the acquisition of CPG network control signals for precise steering gear control. The Arduino panel based on the ATMEGA328 microcontroller, is good at reading data from the water quality sensor module. These data include key parameters, such as water temperature and pH levels. The board controls six controllable PWM output ports to manage the steering engines in the pectoral fin swing mechanism, and uses a timer to control the steering engine in the caudal fin mechanism accurately.

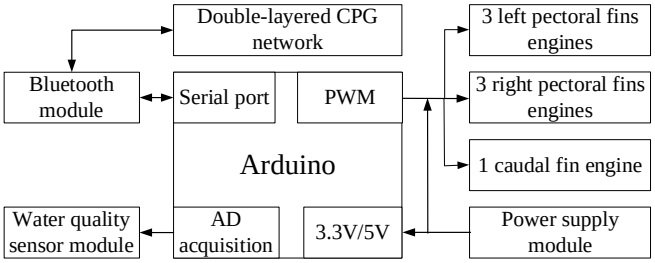

Fig. 5. The schematic diagram of the overall control system

There are six steering gears in the pectoral fin mechanism of the ray robot. The steering gear is selected for actuating the pectoral fin swing mechanism. The controllable angle range of the gear is 180°, and the drive mode is PWM. The actuator drive circuit of the caudal fin is similar to that of the pectoral fin. For seamless communication between the ray robot and a computer, a JDY-31 Bluetooth module is integrated, facilitating remote monitoring and control. In order to conduct comprehensive water quality analysis, the robot is equipped with a TDS sensor, including signal processing module and the sensor probe. TDS value is an important indicator of water purity, expressed by mg/l or EC values.

IV. Research on Motion Control of the Bionic Ray Robot Based on a CPG Network

The control method based on CPG exhibits good robustness and can generate stable periodic signals to regulate the rhythmic swimming of the robot. By adopting the CPG-based motion control strategy, the bionic robot is capable of executing a multitude of rhythmic swimming patterns, such as adjusting speed, body swing and fin flapping. These capabilities not only facilitate a more authentic simulation of fish-like motion behaviors but also significantly enhance the overall motion performance and interaction ability of the robot.

A. Research and design of the CPG network control hierarchy structure of the bionic ray robot

CPG network establishes different topological structures through various connection modes among neurons, specifically chain and network configurations. In the chain structure, neurons are interconnected only with their immediate neighbors, facilitating the gradual transmission of phase changes sequentially. On the contrary, the network structure involves extensive coupling among all neurons, making it suitable for controlling complex rhythmic movement. Each pectoral fin of the designed ray robot is composed of three articulated joints, with the phase at each joint progressively varying from the base to the tip along the longitudinal axis of the fin. For this purpose, a chain-like CPG network is implemented.

The proposed double-layered CPG network is derived from a single-layer semi-central architecture and adds a pattern layer governed by the rhythm layer. To fulfill the functional demands at each level of the double-layered CPG network, three key considerations are addressed. Firstly, the CPG neurons in the rhythm layer must establish phase relationships between functional units. Secondly, the CPG neurons in the pattern layer correspond to joints in each functional unit one by one to control the phase relationships and trajectories of the joint movement. Thirdly, the output

signal of the pattern layer should be based on the output signal of the rhythm layer, and the rhythm layer signals should remain unaffected by the pattern layer signals.

Accordingly, a control scheme for the double-layered CPG network has been developed, as illustrated in Fig. 6. The control scheme comprises a rhythm layer and a pattern layer to regulate the seven joints of the bionic ray robot. The rhythm layer consists of three CPG neurons, each responsible for regulating the phase relationships among the joint groups of the pectoral fins and the caudal fin. Each pectoral fin joint group comprises three joints, and the caudal fin group contains a single joint. The pattern layer includes two groups of neurons and a single neuron, corresponding to each joint within the above three joint groups, which generate control signals for the swinging mechanism.

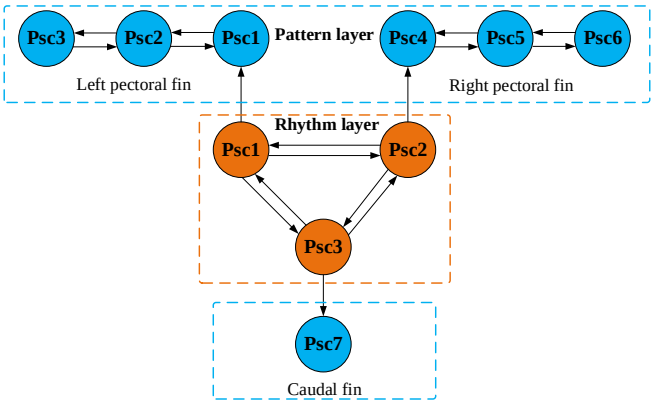

Fig. 6. Structure of the double-layered CPG network

B. Construction and analysis of the double-layered CPG network model

Kuramoto oscillator is famous for its ability to clarify the phase coupling relationships among oscillators in the system. Its parameters are adjustable, which is very important for generating stable control signals [27]. In this paper, the Kuramoto oscillator model is adopted as a replacement for biological neurons, enabling effective manipulation and fine-tuning of the motion behavior. For each complete motion cycle around the limit cycle, the phase of a self-excited nonlinear oscillator advances by 2π when its output signal influences each joint. The phase of each joint is represented by θ_i, and the intrinsic frequency of the oscillator on the limit cycle is denoted as ω_i, which quantifies the rate at which the phase changes. Therefore, in a system composed of same nonlinear oscillators that are not interconnected, the dynamic equation controlling the movement of the i-th oscillator along the limit cycle can be expressed as follows.

$$\dot{\theta}_i = \omega_i \tag{2}$$

When there exist coupling relationships among oscillators, the dynamic equation can be expressed as follows.

$$\dot{\theta}_i = \omega_i + c\sum_{j=1}^{N} a_{ij} H\left(\theta_j - \theta_i\right) \tag{3}$$

where c represents the coupling strength between oscillators. $H(\cdot)$ denotes the coupling function, and a_{ij} stands for the coupling coefficient between oscillators. For coupled oscillators, $a_{ij}=a_{ji}=1(i\neq j)$, whereas for uncoupled ones, $a_{ij}=a_{ji}=0(i\neq j)$.

The Kuramoto oscillator uses the sine coupling function $\sin(\cdot)$, and its dynamic model can be expressed as follows.

$$\dot{\theta}_i = \omega_i + \frac{r}{n}\sum_{j=1}^{N} \sin\left(\theta_j - \theta_i\right) \tag{4}$$

where r represents the coupling strength between the oscillators, and n denotes the number of nonlinear oscillators in the system.

When the motion control system achieves synchrony, the Kuramoto oscillators is synchronized, which is inconsistent with the behavior of neurons during the rhythmic movement of rays. In order to eliminate this discrepancy, a specific phase offset is introduced to create a controlled phase among the oscillators. This adjustment makes the model more reflective of the rhythm control signals generated by biological neurons. The improved Kuramoto model can be expressed as follows.

$$\dot{\theta}_i = \omega_i + \frac{r}{n}\sum_{j=1}^{N} \sin\left(\theta_j - \theta_i - \varphi_{ij}\right) \tag{5}$$

$$\dot{\theta}_i = 2\pi\omega + \sum_{j=1}^{N} w_{ij} \sin\left(\theta_j - \theta_i - \varphi_{ij}\right) \tag{6}$$

where the model parameter coupling strength w_{ij} determines the synchronous convergence speed of CPG neurons, with larger values enhancing the convergence velocity. ω and φ_{ij} determine the angular frequency and phase difference of the output signal of the CPG neuron respectively. θ represents the state variable of the CPG neuron phase. To streamline the above model, a consistent coupling strength is allocated to each neuron, ensuring that φ_{ij} is equal to φ_{ji}.

This model is especially suitable for CPG neurons in the rhythmic layer, and only focuses on establishing phase relationships among the neurons. On the contrary, CPG neurons in the pattern layer not only establish phase relationships, but also determine the joint trajectories. The neuron model is presented as follows.

$$\begin{cases} \dot{\theta}_i = 2\pi\omega + \sum_{j=1}^{N} w\sin\left(\theta_j - \theta_i - \varphi_{ij}\right) \\ \varphi_i = A\sin\theta_i + \gamma \end{cases} \tag{7}$$

The parameter ω is set to 1, and w_{ij} is set to 200. φ_{ij} is assigned as $\pi/2$ or $-\pi/2$ based on different neuron objects, and that of the caudal fin is designated as $\pi/4$. The parameter values of the CPG neuron models in the pattern layer are set similar to those in the rhythm layer. The sigmoid function is introduced to make the output signal more ordered. In the subsequent experiments, the Sigmoid function was added.

$$\varphi_i = \left(1+\mathrm{e}^{-\tau(t-\sigma)}\right)^{-1}\left(A\sin\theta_i + \gamma\right) \tag{8}$$

where τ is the time constant of the output signal masking

function, and σ is the center position of the output signal masking function.

C. The control algorithm of the movements

During the straight movement of the ray robot, the left and right pectoral fins demonstrate equal amplitude and frequency. When configuring the parameters of the CPG network, the input waveform parameters for the pectoral fins are assigned equal values in amplitude and frequency, but the phase difference is π. The simulation results of the straight movement of the bionic ray robot are shown in Fig. 7. The output signals change smoothly without sudden changes, which is beneficial to protect the motors from damage. And Fig. 7. further illustrates the importance of introducing the sigmoid function to avoid simulation failure caused by sudden change of angle. Because the caudal fin only plays a role in stabilizing the balance of the fish, the amplitude and frequency values are set relatively small. Rays mainly rely on the swing of the pectoral fin to generate the forward propulsion. The amplitude and frequency are several times higher than the set value of the caudal fin, and the left and right pectoral fins are symmetrical with respect to the *x*-axis.

During the turning movement of the ray robot, the swing amplitude and frequency between the left and right pectoral fins are inconsistent. When the robot turns left, the right pectoral fin shows a larger swing amplitude and a higher frequency compared to the left pectoral fin. Conversely, when the robot turns right, these characteristics are swapped. Therefore, when configuring the CPG network parameters in the Simulink model, the amplitude and frequency of the input waveform parameters for each pectoral fin must be fine-tuned and optimized accordingly. The final adjustments should be modified based on the analysis in simulation software. The simulation results of the turning movement are shown in Fig. 8. In order to emphasize the visibility of turning effects, it is very important to reduce the influence of the pectoral fins on one side by reducing the amplitude and frequency. The settings of the caudal fin should follow the principles applied in the straight movement.

During the diving movement of the ray robot, the amplitude and frequency of the left and right pectoral fins are the same, but the frequency is higher than that of the straight movement. When configuring the parameters of the CPG

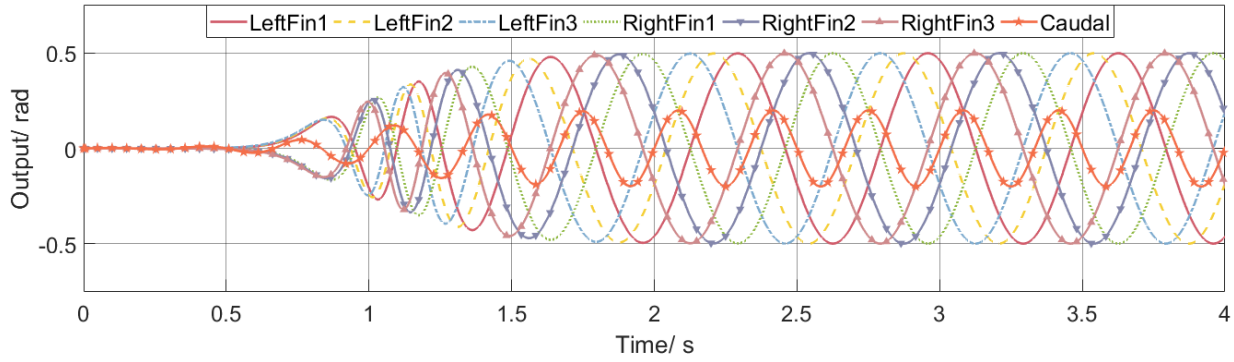

Fig. 7. The simulation results of straight movement

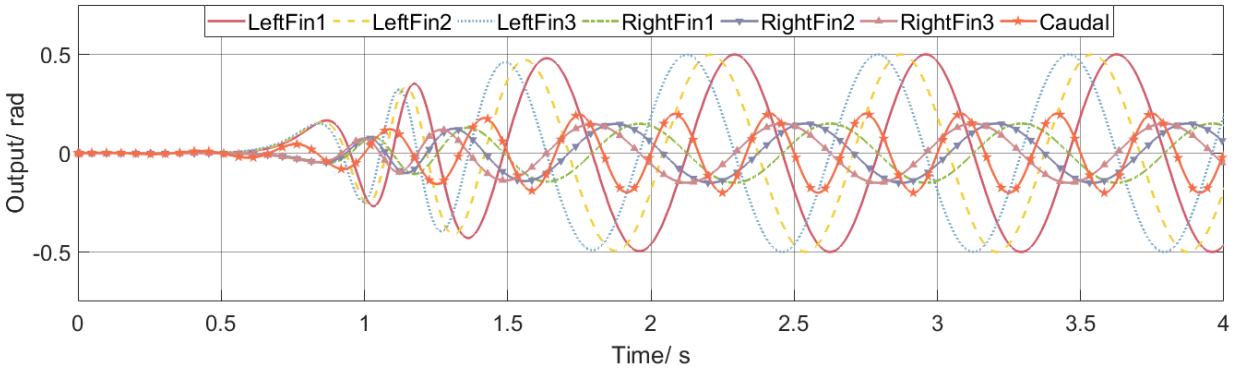

Fig. 8. The simulation results for turning movement of the bionic ray robot

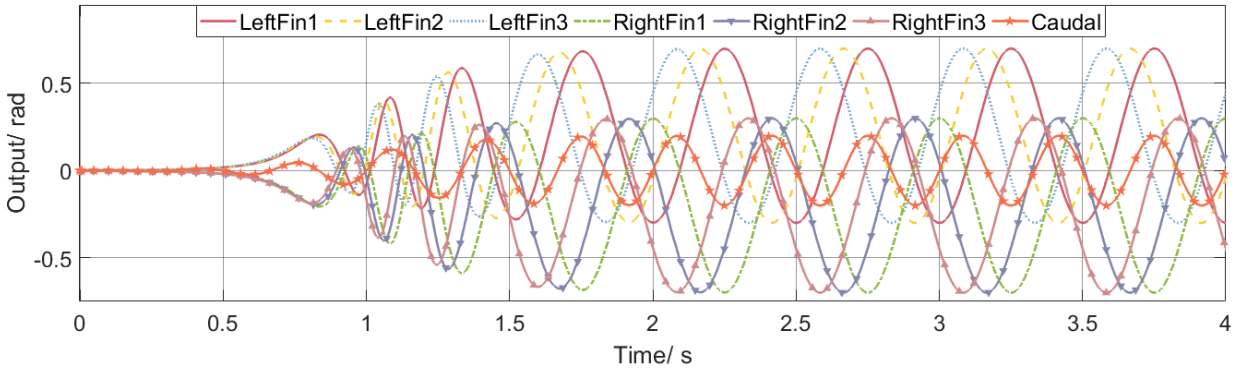

Fig. 9. The simulation results of the diving movement of the bionic ray robot

network, it is necessary to set equal values for the amplitude and frequency of the input waveform parameters of the two pectoral fins. However, the frequency should be set higher than that used during straight movement, and a phase differenceπ must still be maintained. The simulation results of the diving movement are shown in Fig. 9. It can be observed from the figure that some waveforms on one side of the pectoral fin overlap due to the increase of frequency. In order to achieve the desired diving effect, the overall waveform is shifted to one side of the axis in the parameter setting, that is, the waveform of the left pectoral fin is raised to the upper side of the axis, while the right pectoral fin moves downward due to the phase difference waveform. This arrangement ensures that the upward swing amplitude of the pectoral fin is greater than their downward swing amplitude, leading to rapid diving.

V. Simulation and Experimental Analysis of the Bionic Ray Robot

After constructing the CPG network model of the bionic ray robot, the feasibility and the performances of the model are verified by simulations and experiments. The physical characteristics of the underwater environment are simulated in Webots software. The CPG-based control method is implemented through MATLAB software. Finally, the prototype with a Bluetooth communication module is built. The functions of the ray robot are demonstrated.

A. Simulations of the bionic ray robot based on Webots and Simulink

The fish body, inclding three steering gears and their respective brackets for the left and right pectoral fins, as well as the caudal fin, are imported into the Webots simulation software. The simulation structure of the ray robot in Webots software is shown in Figure 10. Taking the right pectoral fin as an example, HingeJoint is added to make the steering gear operate. In the setting of JointParameters, Axis is the rotation axis of the steering gear, and Anchor is the origin of the coordinate axis. By setting these two values, we can determine the rotation axis around which the steering gear runs. BoundingObject and Physics are set for the physical boundaries and physical properties, respectively, to avoid model penetration. The selection RotationMotor in the set of Device is chosen to produce the effect of a rotating motor. If all parameters are set successfully, the steering gear can be rotated by modifying the position value. The set of the caudal fin is consistent with that of the pectoral fin.

Once a co-simulation environment between Webots and MATLAB is successfully established, the multi-modal optimization of the bionic ray robot can be realized by adjusting parameters such as amplitude and frequency in Simulink. The simulated screenshots of the straight swimming of the bionic ray robot in a wave-free environment are presented in Figure 11(a). By observing the swimming posture from a top view, it can be observed that the robot mainly generates propulsion mainly through vertical swing of its pectoral fins and slight fluctuation of its caudal fin, so as to glide smoothly. This mode of movement closely mimics the behavior of real rays during straight swimming.

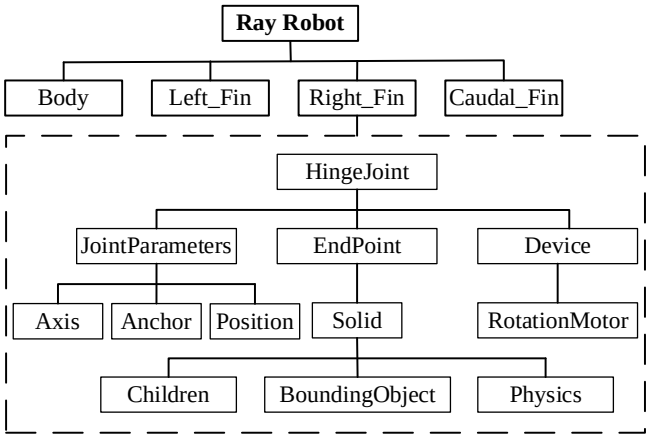

Fig.10 The structure of the ray robot in Webots

The simulation screenshots of the turning movement in a wave-free environment are shown in Fig. 11(b). By observing the swimming posture of the ray robot from a top-down perspective, it can be observed that the body maintains an impressively stable trajectory during the right turn. The main mechanism of turning movement is to realize the overall direction deviation and propulsion by adjusting the swing amplitude difference between the left and right pectoral fins and slight caudal fin swing. This special motion posture is in harmony with the inherent characteristics displayed by real rays when executing turns.

The simulation screenshots of the diving movement in a wave-free environment are illustrated in Fig. 11(c). By observing the dynamic diving process of the ray robot from a lateral perspective, it can be observed that the pectoral fin and caudal fins swing upward more than downward. Considering the influence of gravity on the robot itself, this oscillating

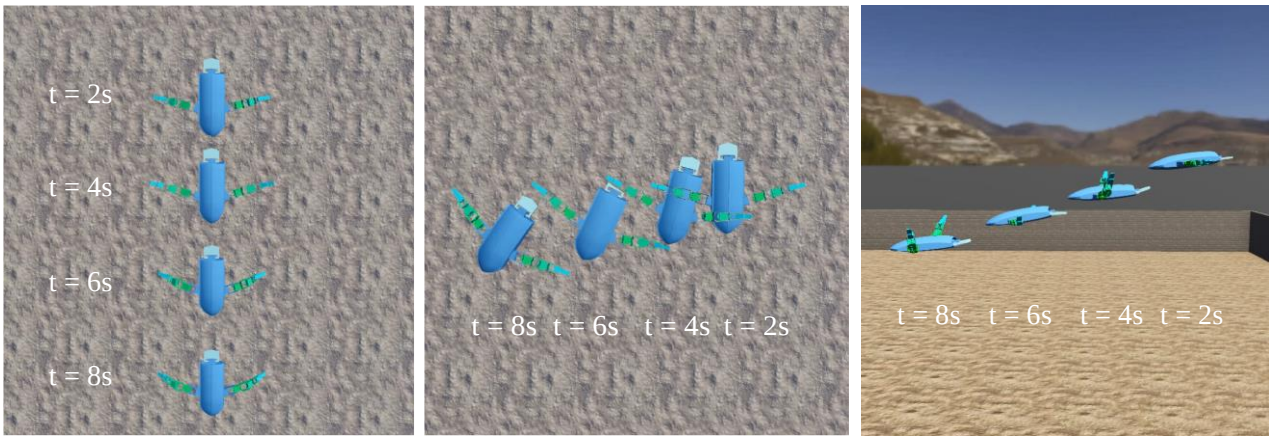

(a) The straight movement (b) The turning movement (c) The diving movement

Fig. 11. The simulation screenshots in the wave-free environment

movement helps to sink synchronously, which effectively imitates the natural diving posture of real stingrays.

B. Experiments of water quality detection

According to the TDS hardness scale, the measured values between 0 and 89 ppm represent very soft water, while a range of 90 to 159 ppm denote soft water. Water with a TDS level between 160 and 229 ppm is considered to be medium hard, while water with a TDS level between 230 to 339 ppm is classified as moderately hard. Any reading from 340 to 534 ppm indicates the water is hard water, and any value above 535 ppm indicates that water is very hard. As shown in Fig. 12, two samples of tap water with different levels of purity were analyzed using a TDS water quality sensor to determine the concentration of dissolved solids and to evaluate the overall purity of the water.

(a)Tap water (b) Tap water with sand

Fig. 12. Two samples of tap water with varying degrees of purity

The results of the two water samples are presented in Fig.13. Fig.13(a) reveals that the tap water keeps a stable TDS value of around 134 ppm, which classifies the water as soft water. On the contrary, Fig.13(b) shows that tap water containing suspended sand exhibits fluctuating TDS values ranging from 180 ppm to 185 ppm. This variability is attributed to the non-uniform distribution of solid substances within the liquid, leading to its classification as moderately hard water.

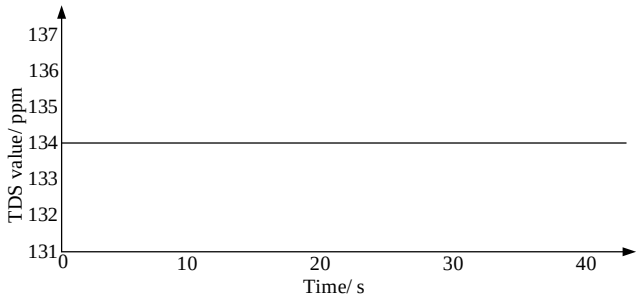

(a) Tap water

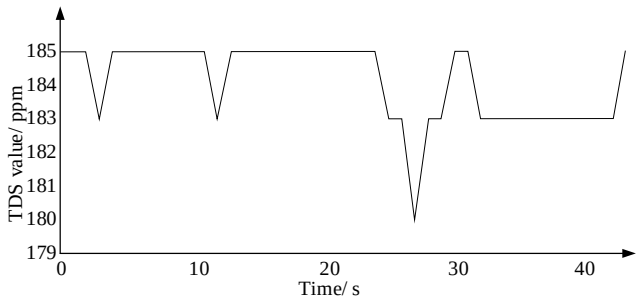

(b) Tap water with sand

Fig. 13. Measurement results of tap water with varying degrees of purity

C. Experiments on the locomotion of the bionic ray robot

The experimental sequence diagrams of the bionic ray robot during the straight movement over a cycle are shown in Fig. 14(a). It is obvious from the figure that the swing amplitude and frequency of the left and right pectoral fins are synchronous.

The experimental sequence diagrams of the bionic ray robot during the turning movement in a cycle are shown in Fig. 14(b). Taking the right turn of the ray robot as an example, it is noticeable that the swing amplitude of the left pectoral fin is much greater than that of the right pectoral fin. In addition, compared with the right side, the swinging frequency of the left pectoral fin is slightly increased.

The experimental sequence diagrams of the diving movement in a cycle are shown in Fig. 14(c). It is evident from the figure that, in contrast to straight movement, the swing amplitudes of both the left and right pectoral fins during diving are significantly greater than those observed during straight movement.

By analyzing the multi-modal motion performance of the bionic robotic ray under different parameters of the CPG controller, the results demonstrate that the proposed double-layered CPG control method not only facilitates versatile locomotion but also exhibits good robustness.

VI. Conclusion and Future Work

This paper introduces the design of a bionic ray robot, which mimics the movement of natural rays through pectoral fin swing propulsion. Firstly, the biological characteristics of natural rays are analyzed, and the mechanical structure of the bionic ray robot is designed. Secondly, a control method based on a double-layered CPG is proposed. This approach builds a CPG model for the bionic ray robot using Kuramoto oscillators and integrates a pattern layer based on a traditional single-layer semi-central configuration to accomplish rhythm layer control. Finally, a ray robot prototype is made, and Bluetooth remote control and water quality detection experiments are realized. The feasibility and correctness of the double-layered CPG motion control method for the bionic ray robot are verified through simulations and experiments. By adjusting the parameters of CPG model, three motion modes including straight movement, turning movement, and dynamic diving/floating movement are controlled effectively. This research has important theoretical and practical significance in the field of biological motion control and bionic robot.

However, due to the limitations of experimental conditions, there are several shortcomings in this paper. The structure and motion characteristics of rays are simplified, which reduces the biomimicry of the robotic rays. Future research should focus on further optimizing and refining the algorithm parameters to adapt to diverse underwater environments and improve the performance and adaptability of the system.

References

[1] Q. Liu, H. Chen, Z. Wang, Q. He, L. Chen, W. Li, R. Li, W. Cui, “A manta ray robot with soft material based flapping wing,” *Journal of Marine Science and Engineering*, vol.10, no.7, pp.962, 2022.

[2] Y. Cai, S. Bi, G. Li, H. P. Hildre, H. Zhang, “From natural complexity to biomimetic simplification: the realization of bionic fish inspired by the cownose ray,” *IEEE Robotics & Automation Magazine*, vol.26, no.3, pp.27-38, 2019.

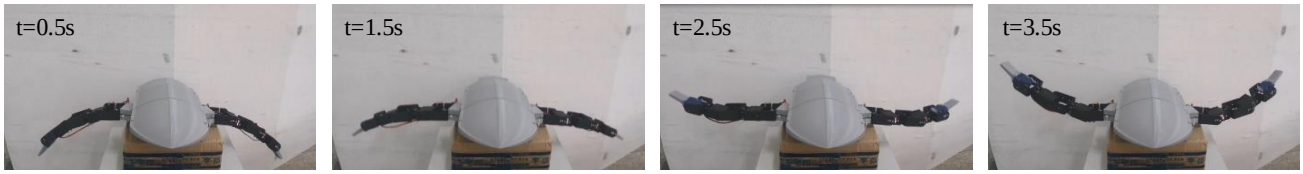

(a) The straight movement

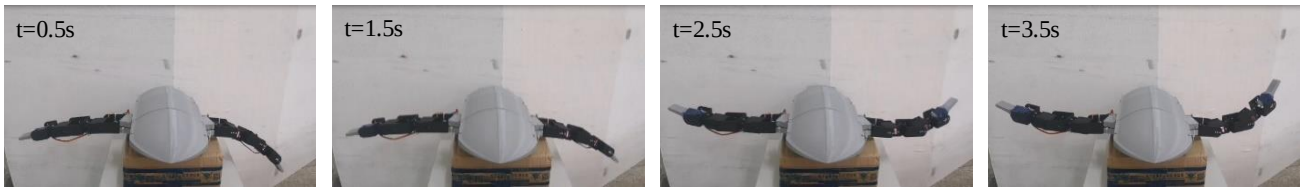

(b) The turning movement

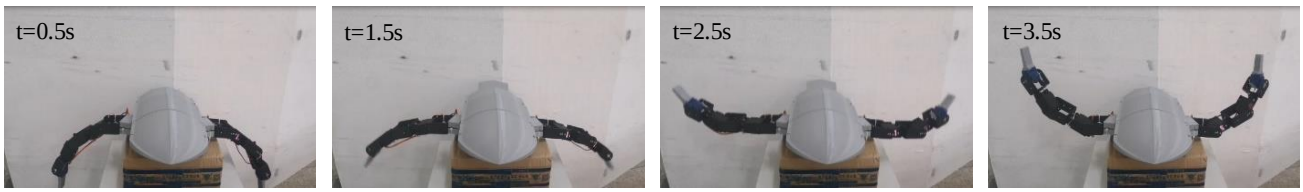

(c) The diving movement

Fig. 14. The experimental sequence diagrams

[3] F. E. Fish, A. Kolpas, A. Crossett, M. A. Dudas, K. W. Moored, "Bart-Smith H. Kinematics of swimming of the manta ray: three-dimensional analysis of open-water maneuverability," *Journal of Experimental Biology*, vol.221, no.6, pp.10, 2018.

[4] Z. Yu, K. Li, Y. Ji, S. Yang, "Fast motion performance of a bionic ray robot with serial pectoral fins," *IEEE Robotics and Automation Letters*, vol.8, no.11, pp.7218-7225, 2023.

[5] W. Cui, L. Lian, P. Guang, "Frontiers in deep-sea equipment and technology," *Journal of Marine Science and Engineering*, vol.11, no.4, pp.715, 2023.

[6] Z. Zhao, L. Dou, "Effects of the structural relationships between the fish body and caudal fin on the propulsive performance of fish," Ocean Engineering, pp.186, no.15, pp.106117, 2019.

[7] M. S. A. M. Nor, M. Aliff, N. Samsiah, "A review of a biomimicry swimming robot using smart actuator," *International Journal of Advanced Computer Science and Applications*, vol.12, no.11, pp.395-405, 2021.

[8] Z. Wang, C. Dong, Z. Zhang, Q. Tian, A. Sun, L. Yuan, L. Zhang, "Review of multi-fin propulsion and functional materials of underwater bionic robotic fish," *Proceedings of the Institution of Mechanical Engineers, Part C: Journal of Mechanical Engineering Science*, pp.236, no.13, pp.7350-7367, 2022.

[9] M. S. Triantafyllou, F. S. Hover, A. H. Techet, D. K. P. Yue, "Review of hydrodynamic scaling laws in aquatic locomotion and fishlike swimming," *Applied Mechanics Reviews*, vol.58, pp.226–237, 2005.

[10] G. Ozmen Koca, C. Bal, D. Korkmaz, M. C. Bingol, M. Ay, Z. H. Akpolat, S. Yetkin, "Three-dimensional modeling of a robotic fish based on real carp locomotion," *Applied Sciences*, vol.8, pp.180, 2018.

[11] D. S. Barrett, "The design of a flexible hull undersea vehicle propelled by an oscillating foil," *Doctoral dissertation*, Massachusetts Institute of Technology, 1994.

[12] C. Zhou, K. H. Low, "Better endurance and load capacity: an improved design of manta ray robot (RoMan-II)," *Journal of Bionic Engineering*, vol.7, no.S4, pp.S137-S144, 2010.

[13] K. H. Low, C. Zhou, G. Seet, S. Bi, Y. Cai, "Improvement and testing of a robotic manta ray (RoMan-III)," Proceedings of IEEE International Conference on Robotics and Biomimetics, 07-11 December, 2011, pp.1730-1735.

[14] Z. Chen, T. I. Um, J. Zhu, H. Bart-Smith, "Bio-inspired robotic cownose ray propelled by electroactive polymer pectoral fin," *ASME International Mechanical Engineering Congress and Exposition*, vol.54884, pp.817-824, 2011.

[15] I. Glushko, E. Olenew, M. Komar, L. Kniese, R. Sokolovskyi, O. Kebkal, R. Bannasch, K. Kebkal, "Software control architecture for the boss manta ray AUV actuation system," Proceedings of 2018 IEEE/OES Autonomous Underwater Vehicle Workshop, Porto, Portugal, 06-09 November, 2018, pp. 1-5.

[16] Y. Cai, S. Bi, L. Zheng, "Design optimization of a bionic fish with multi-joint fin rays," *Advanced Robotics*, vol.26, no.1-2, pp.177-196, 2012.

[17] H. Zhu, H. Xing, J. Zhu, P. Zhang, "Design of Fuzzy Gait Control Algorithm for Multi-legged Hydraulic Robot," *IAENG International Journal of Computer Science*, vol. 50, no.3, pp1042-1049, 2023.

[18] A. J. Ijspeert, "Central pattern generators for locomotion control in animals and robots: a review," *Neural Networks*, vol.21, no.4, pp.642–653, 2008.

[19] E. M. R. Mesa, J. A. Hernandez-Riveros, "Handling the transition in the locomotion of an articulated quadruped robot by adaptive CPG," *IAENG International Journal of Computer Science*, vol. 47, no.4, pp792-804, 2020.

[20] X. Liao, C. Zhou, J. Wang, J. Fan, Z. Zhang, "A wire-driven elastic robotic fish and its design and CPG-based control," *Journal of Intelligent & Robotic Systems*, vol.107, pp.4, 2023.

[21] Z. Cui, L. Li, Y. Wang, Z. Zhong, J. Li, "Review of research and control technology of underwater bionic robots," *Intelligent Marine Technology and Systems*, vol.1, no.1, pp.7, 2023.

[22] M. Wang, H. Dong, X. Li, Y. Zhang, J. Yu, "Control and optimization of a bionic robotic fish through a combination of CPG model and PSO," *Neurocomputing*, vol.337, pp.144-152, 2019.

[23] V. D. Nguyen, Q. D. Tran, Q. T. Vu, V. T. Duong, H. H. Nguyen, T. T. Hoang, T. T. Nguyen, "Force optimization of elongated undulating fin robot using improved PSO-based CPG," *Computational Intelligence and Neuroscience*, pp.2763865, 2022.

[24] Y. Zhang, S. Wang, X. Wang, Y. Geng, "Design and control of bionic manta ray robot with flexible pectoral fin," Proceedings of 2018 IEEE 14th International Conference on Control and Automation, Anchorage, USA, 12-15 June, 2018, pp.1034-1039.

[25] C. Bal, G. O. Koca, D. Korkmaz, Z. H. Akpolat, M. Ay, "CPG-based autonomous swimming control for multi-tasks of a biomimetic robotic fish," Ocean Engineering, vol. 189, pp.106334, 2019.

[26] L. J. Rosenberger, "Pectoral fin locomotion in batoid fishes: undulation versus oscillation," *Journal of Experimental Biology*, vol.204, no.2, pp.379-394, 2001.

[27] R. Heliot, B. Espiau, "Multisensor input for CPG-based sensory-motor coordination," *IEEE Transactions on Robotics*, vol.24, pp.191-195, 2008.